

Anisotropic magnetic and superconducting properties of aligned weak-ferromagnetic superconductor $\text{RuSr}_2\text{RCu}_2\text{O}_8$ (R = rare earths)

B. C. Chang, C. H. Hsu, M. F. Tai, and H. C. Ku*

Department of Physics, National Tsing Hua University, Hsinchu 30013, Taiwan, Republic of China

Y. Y. Hsu

Department of Physics, National Taiwan Normal University, Taipei 11677, Taiwan, Republic of China

(Dated: November 6, 2018)

The powder alignment method is used to investigate the anisotropic physical properties of the weak-ferromagnetic superconductor system $\text{RuSr}_2\text{RCu}_2\text{O}_8$ (R = Pr, Nd, Sm, Eu, Gd, $\text{Gd}_{0.5}\text{Dy}_{0.5}$). The $\text{RuSr}_2\text{GdCu}_2\text{O}_8$ Ru-1212 cuprate is a weak-ferromagnetic superconductor with a magnetic ordering of Ru moments at $T_N(\text{Ru}) = 131$ K, a superconducting transition in the CuO_2 layers at $T_c = 56$ K, and a low temperature Gd antiferromagnetic ordering at $T_N(\text{Gd}) = 2.5$ K. Due to weak magnetic anisotropy of this tetragonal system, highly c -axis aligned microcrystalline powder (diameter $\sim 1\text{-}10\ \mu\text{m}$) in epoxy can be obtained only for R = Eu and Gd through the field-rotation powder alignment method where c -axis is perpendicular to the aligned magnetic field $B_a = 0.9$ T and parallel to the rotation axis. For smaller rare earth compound R = $\text{Gd}_{0.5}\text{Dy}_{0.5}$, powder alignment can be achieved using the simple field powder alignment method where c -axis is partially aligned along the aligned magnetic field. No powder alignment can be achieved for larger rare earths R = Pr, Nd or Sm due to the lack of magnetic anisotropy in these compounds. The anisotropic temperature dependence of magnetic susceptibility for the c -axis aligned powders exhibit weak anisotropy with $\chi_c > \chi_{ab}$ at room temperature due to anisotropic rare earth, Eu and Gd, contribution and crossover to $\chi_c < \chi_{ab}$ below 190 K where strong Ru anisotropic short-range exchange interaction overtakes the rare earth contribution. Anisotropic diamagnetic superconducting intragrain shielding signal of aligned microcrystalline $\text{RuSr}_2\text{GdCu}_2\text{O}_8$ powder-in-epoxy below vortex lattice melting temperature at 39 K in 1-G field is much weaker than the intergrain polycrystalline bulk sample signal due to the small grain size ($d \sim 1\text{-}10\ \mu\text{m}$), long penetration depth ($\lambda_{ab} \sim 0.55\ \mu\text{m}$, $\lambda_c \sim 0.66\ \mu\text{m}$) and the two-dimensional (2D) character of CuO_2 layers.

PACS numbers: 74.72.-h, 74.70.Pq, 75.30.Gw

I. INTRODUCTION

Magnetic superconductivity has attracted much research attention since it was reported in the strongly-correlated $\text{RuSr}_2\text{RCu}_2\text{O}_8$ Ru-1212 cuprate system (R = Sm, Eu, Gd, Y) with the tetragonal space group $P4/\text{mbm}$.^{1,2,3,4,5} The Ru magnetic moments order weak-ferromagnetically (WFM) with ordering temperature $T_N(\text{Ru}) \sim 130$ K. High- T_c superconductivity occurs in the quasi-2D CuO_2 bi-layers from doped holes with maximum superconducting transition onset $T_c(\text{onset}) \sim 60$ K for R = Gd and coexists with the WFM order. A crossover from anisotropic 2D-like to less-anisotropic 3D-like structure was observed near R = Sm, along with a metal-insulator transition. No superconductivity can be detected for the Mott insulators R = Pr and Nd.

Since the oxygen content for all samples is close to eight after oxygen annealing, the variation of T_c with rare-earth ions indicates a self-doping of electrons from CuO_2 layers to RuO_6 layers. Such self-doping creates hole carriers in CuO_2 layers and conduction electrons in RuO_6 layers. The Ru L_3 -edge X-ray absorption near-edge spectrum (XANES) of $\text{RuSr}_2\text{GdCu}_2\text{O}_8$ indicates that Ru valence is basically at Ru^{5+} ($4d\text{-}t_{2g}^3$, $S = 3/2$) state with small amount ($\sim 20\%$) of Ru^{4+} ($4d\text{-}t_{2g}^4$, $S = 1$ in low spin state) which corresponds to doped electrons.⁶ The

strong antiferromagnetic superexchange interaction between Ru^{5+} moments is responsible for the basic G-type antiferromagnetic order observed in the neutron diffraction study.⁷ The weak ferromagnetic component observed from magnetic susceptibility and NMR spectrum is probably due to weak-ferromagnetic double-exchange interaction through doped conduction electrons in the metallic RuO_6 layers.

Since the magnetic superexchange and double-exchange interaction is anisotropic in general, the study of anisotropic physical properties is crucial for this quasi-2D system. In this report, we align the microcrystalline $\text{RuSr}_2\text{RCu}_2\text{O}_8$ (R = rare earths) powder ($\sim 1\text{-}10\ \mu\text{m}$) in magnetic field to investigate the anisotropic properties.

II. EXPERIMENTAL

The stoichiometric $\text{RuSr}_2\text{GdCu}_2\text{O}_8$ bulk sample was synthesized by the standard solid-state reactions. High-purity RuO_2 (99.99%), SrCO_3 (99.9%), Gd_2O_3 (99.99%) and CuO (99.99%) preheated powders with the nominal composition ratio of Ru:Sr:Gd:Cu = 1:2:1:2 were well mixed and calcined at 960°C in air for 16 hours. The calcined powders were then pressed into pellets and sintered in flowing N_2 gas at 1015°C for 10 hours to form $\text{Sr}_2\text{GdRuO}_6$ and Cu_2O precursors. The sintered pellets

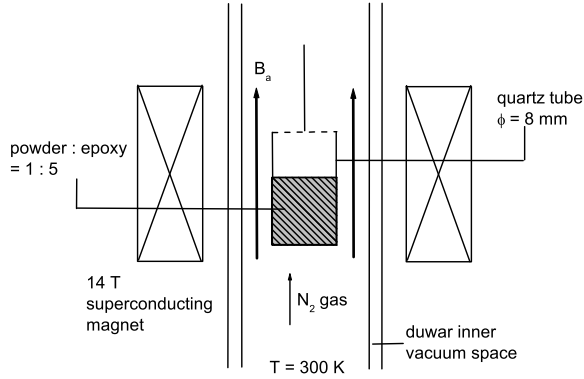


FIG. 1: Schematic diagram for the magnetic field powder alignment method in a 14 T superconducting magnet at 300 K.

were then heated at 1060-1065°C in flowing O₂ gas for 7 days to form the Ru-1212 phase and slowly furnace cooled to room temperature with a rate of 15°C per hour. For powder alignment in magnetic field, samples were ground into powders with an average microcrystalline grain size of 1-10 μm and mixed with epoxy (4-hour curing time) in a quartz tube ($\phi = 8$ mm) with the ratio of powder:epoxy = 1:5 then immediately put into the alignment field environments (simple field or rotation-field alignment).

III. RESULTS AND DISCUSSION

For simple powder alignment, the mixture was placed in a 14-T superconducting magnet at room temperature in flowing N₂ gas and slowly hardened overnight as shown in figure 1. The powder X-ray diffraction pattern of three typical aligned powder-in-epoxy samples RuSr₂RCu₂O₈ (R = Sm, Eu, Gd_{0.5}Dy_{0.5}) are shown collectively in figure 2. For R = Sm (as well as for R = Pr and Nd), no magnetic alignment can be achieved. The lack of magnetic anisotropy may closely relate to the variation of tetragonal lattice parameters where $c/3 \sim a/\sqrt{2}$ for R = Sm with $a = 0.5448$ nm and $c = 1.1560$ nm (space group P4/mbm) as shown in figure 3. For R = Eu (as well as for R = Gd), partial ($\sim 90\%$) ab -plane aligned along alignment magnetic field B_a is observed through the appearance of enhanced $(hk0)$ diffraction lines. A small amount of SrRuO₃ impurity is presented. The ab -plane alignment may be due to the fact that $c/3 > a/\sqrt{2}$ for R = Eu ($a = 0.5435$ nm, $c = 1.1572$ nm). For metastable compound R = Gd_{0.5}Dy_{0.5} near the phase boundary with some unreacted precursor Sr₂RRuO₆, partially c -axis alignment along B_a is detected with enhanced $(00l)$ lines due to $c/3 < a/\sqrt{2}$ in this compound ($a = 0.5426$ nm, $c = 1.1508$ nm).

The phase diagram in figure 3 indicates a structural

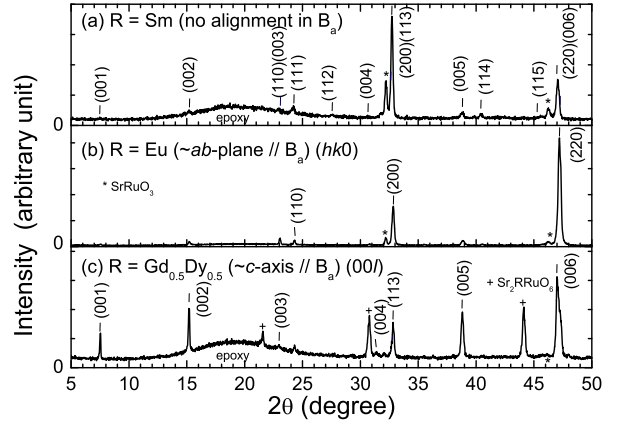


FIG. 2: Powder X-ray diffraction patterns for RuSr₂RCu₂O₈ aligned powder. (a) R = Sm, (b) R = Eu, (c) R = Gd_{0.5}Dy_{0.5}.

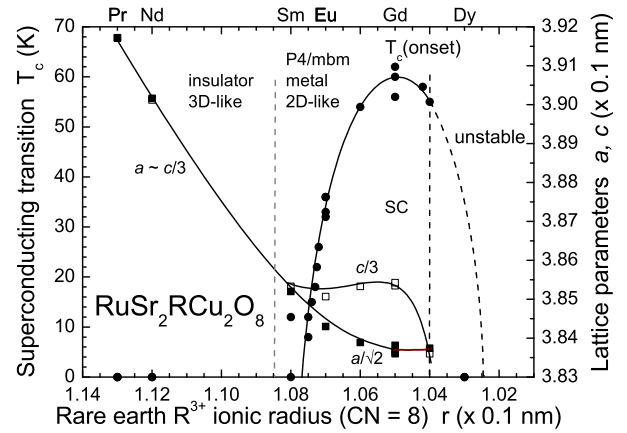


FIG. 3: The variation of superconducting transition T_c and tetragonal lattice parameters a , c with rare earth ionic radius R^{3+} for RuSr₂RCu₂O₈ system (R = Pr-Dy).

crossover from less-anisotropic 3D-like ($c/3 \sim a$) to anisotropic 2D-like structure ($c/3 \neq a/\sqrt{2}$) near R = Sm, along with an insulator-to-metal transition. Superconductivity appears only in the quasi-2D metallic region with resistivity onset transition temperature $T_c \sim 0$ for R = Sm, $T_c = 36$ K for R = Eu, $T_c = 56$ K for Gd, and $T_c = 55$ K for metastable R = Gd_{0.5}Dy_{0.5}.

For R = Eu with ab -plane aligned along B_a , c -axis can be in any direction within the plane perpendicular to B_a . To obtain the c -axis aligned powder, a field-rotation alignment method is used as shown in figure 4. Since ab -plane is fixed along B_a , the rotation of quartz tube (10 rpm) perpendicular to B_a forces the microcrystalline c -axis to have no choice but to be aligned along the rotation axis. The powder X-ray diffraction patterns of RuSr₂EuCu₂O₈ random powder (hkl), partially ab -plane

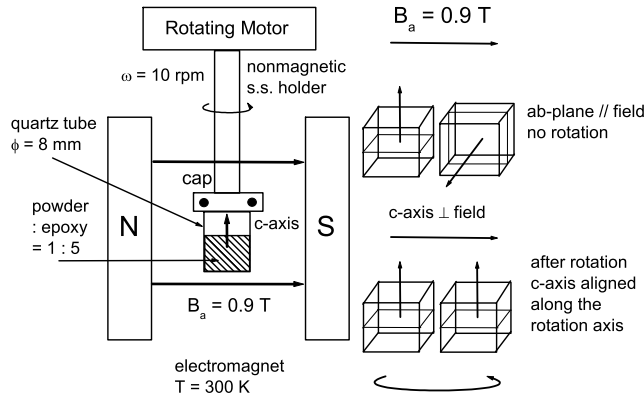


FIG. 4: Schematic diagram for the field-rotation powder alignment method with c -axis perpendicular to aligned magnetic field and along the rotation axis.

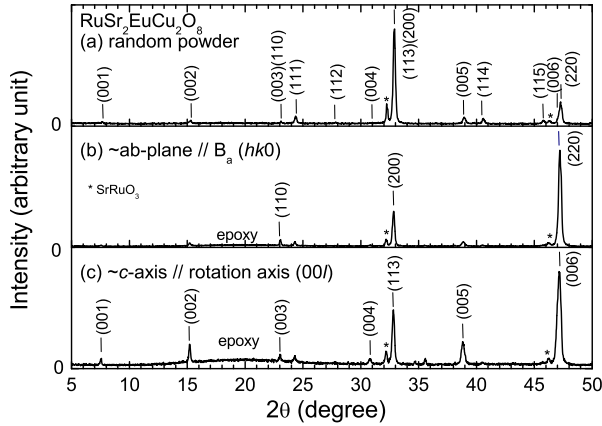


FIG. 5: powder X-ray diffraction patterns for $\text{RuSr}_2\text{EuCu}_2\text{O}_8$. (a) random powder, (b) ab -plane aligned along B_a , and (c) c -axis aligned along the rotation axis.

aligned along B_a ($hk0$), and highly c -axis aligned along the rotation axis ($00l$) are shown collectively in figure 5. The relative intensity of the enhanced ($00l$) lines and (113) line indicates a $\sim 90\%$ c -axis alignment in this field-rotation aligned powder-in-epoxy sample.

Figure 6 shows the field dependence of paramagnetic moment of $\text{RuSr}_2\text{GdCu}_2\text{O}_8$ aligned powder up to 7 T at 300 K. Since ab -plane is aligned along the magnetic field in the alignment procedure at room temperature, magnetic anisotropy of $\chi_{ab} > \chi_c$ at 300 K is expected. However, 300 K m - B_a data showed weak magnetic anisotropy with linear paramagnetic magnetic moment $m_{ab} \sim 0.95 m_c$ or susceptibility $\chi = m/B_a$ with $\chi_{ab} < \chi_c$.

The anisotropic temperature dependence of logarithmic

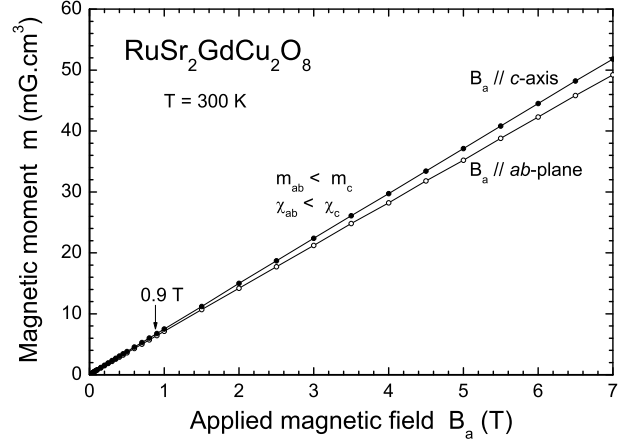


FIG. 6: The field dependence of paramagnetic moment of $\text{RuSr}_2\text{GdCu}_2\text{O}_8$ aligned powder up to 7 T at 300 K. Linear paramagnetic magnetic moment.

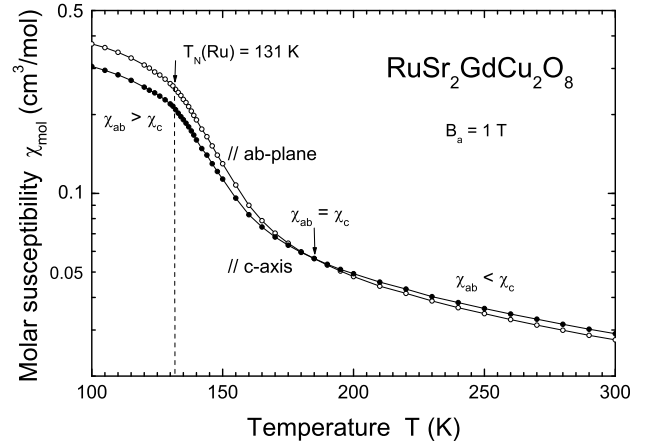


FIG. 7: Temperature-dependence of logarithmic molar magnetic susceptibility χ_{ab} and χ_c .

mic molar magnetic susceptibility of $\text{RuSr}_2\text{GdCu}_2\text{O}_8$ c -axis aligned powder in 1-T applied magnetic field is shown in figure 7. A crossover from $\chi_{ab} < \chi_c$ at 300 K to $\chi_{ab} > \chi_c$ at lower temperature was observed around 185 K, followed by a weak-ferromagnetic ordering at $T_N(\text{Ru}) = 131$ K.

The magnetic anisotropy of $\chi_{ab} < \chi_c$ observed at 300 K is mainly due to the contribution of magnetic Gd^{3+} ions ($J = 7/2$). The anisotropy of $\chi_{ab}(\text{Gd}) < \chi_c(\text{Gd})$ is from the tetragonal GdO_8 cage with anisotropic g -factor $g_{ab} < g_c$, but with little $4f$ wavefunction overlap with the neighbor oxygen $2p$ orbital.

Although there are three types of magnetic moments in this magnetic superconductor: Ru^{5+} ($S = 3/2$) with

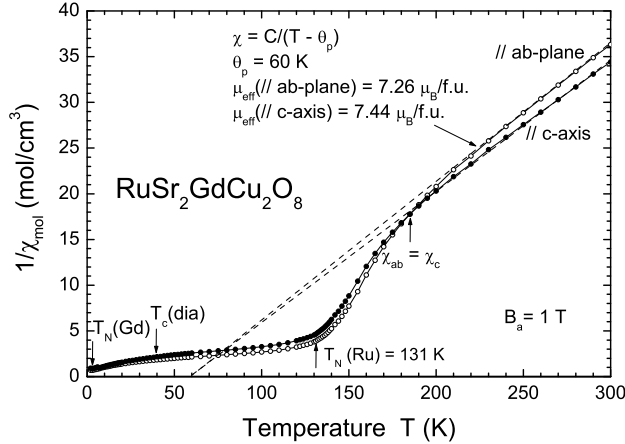


FIG. 8: Reciprocal molar magnetic susceptibility $1/\chi_{ab}$ and $1/\chi_c$ for aligned $\text{RuSr}_2\text{GdCu}_2\text{O}_8$ powder.

doped electrons or Ru^{4+} ($S = 1$), Cu^{2+} ($S = 1/2$) with doped holes, and Gd^{3+} moment ($J = 7/2$), not all moments have the same contribution in powder alignment. In the aligned magnetic field, anisotropic orbital wavefunction is tied to the spin direction, and a strong spin-orbital related short-range anisotropic exchange interaction at 300 K should dominate the magnetic alignment. In the present case, it is believed that Ru moment with the strong short-range anisotropic double-exchange/superexchange interaction along the ab -plane due to the Jahn-Teller distortion of RuO_6 octahedron with $\chi_{ab}(\text{Ru}) > \chi_c(\text{Ru})$ is the dominant factor for ab -plane alignment along B_a at 300 K. The shorter Ru-O(1) bond length in the tetragonal ab -basal plane provides strong $4d_{xy}(\text{Ru})-2p_{x/y}(\text{O}(1))-4d_{xy}(\text{Ru})$ wavefunction overlap. This exchange interaction increases with decreasing temperature, and eventually total $\chi_{ab} > \chi_c$ was observed below 185 K as expected. The weak-ferromagnetic state below 131 K is due to the long range order of this anisotropic double-exchange/superexchange interaction.

The reciprocal molar magnetic susceptibility $1/\chi_{ab}$ and $1/\chi_c$ of $\text{RuSr}_2\text{GdCu}_2\text{O}_8$ aligned powder are shown in figure 8. A Curie-Weiss behavior $\chi = C/(T - \theta_p)$ was observed in the high temperature paramagnetic region above 200 K with a Curie-Weiss intercept $\theta_p = 60$ K for both field orientations and the anisotropic effective magnetic moment $\mu_{eff}^c = 7.44 \mu_B$ per formula unit along the c -axis, and $\mu_{eff}^{ab} = 7.26 \mu_B$ per formula unit along the ab -plane. Diamagnetic superconducting transition $T_c(\text{dia})$ at 39 K and Gd ordering temperature $T_N(\text{Gd}) = 2.5$ K are not clearly seen in this high applied field.

The temperature dependence of logarithmic molar magnetic susceptibility of aligned $\text{RuSr}_2\text{EuCu}_2\text{O}_8$ powder along c -axis and ab -plane in 1-T applied magnetic field are shown in figure 9. Similar to R = Gd com-

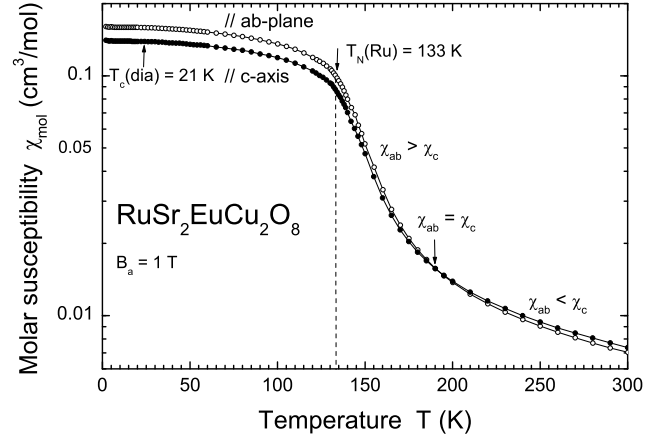


FIG. 9: The temperature-dependence of logarithmic molar magnetic susceptibility χ_{ab} and χ_c of aligned $\text{RuSr}_2\text{EuCu}_2\text{O}_8$ powder in 1 T applied magnetic field.

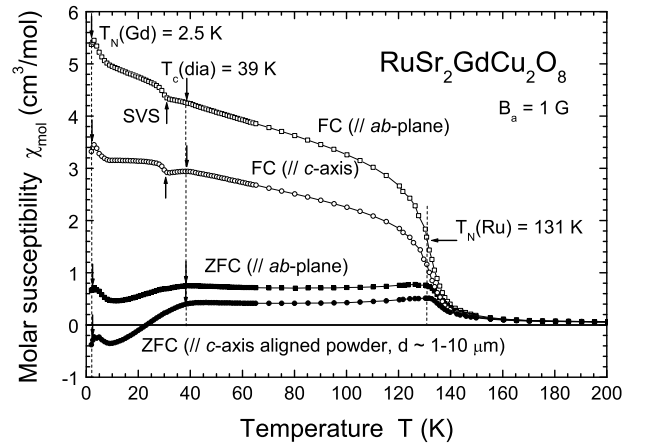


FIG. 10: Low temperature, low field (1-G field-cooled (FC) and zero-field-cooled (ZFC)) anisotropic magnetic and superconducting properties of $\text{RuSr}_2\text{GdCu}_2\text{O}_8$ aligned powder.

pound, weak paramagnetic anisotropy of $\chi_{ab} = 0.95 \chi_c$ was observed at 300 K, and a crossover to $\chi_{ab} > \chi_c$ was detected below 190 K with a weak-ferromagnetic ordering temperature $T_N(\text{Ru}) = 133$ K. Superconducting diamagnetic signal $T_c(\text{dia})$ at 21 K (resistivity zero point) is very weak in large 1-T applied field.

Low temperature, low field (1-G field-cooled (FC) and zero-field-cooled (ZFC)) anisotropic magnetic and superconducting properties of $\text{RuSr}_2\text{GdCu}_2\text{O}_8$ aligned powder are shown in figure 10. A clear weak-ferromagnetic ordering $T_N(\text{Ru})$ at 131 K was observed in all data with $\chi_{ab} > \chi_c$ in the weak-ferromagnetic state for both FC and ZFC measurements. A superconducting diamagnetism setting in at the vortex melting temperature

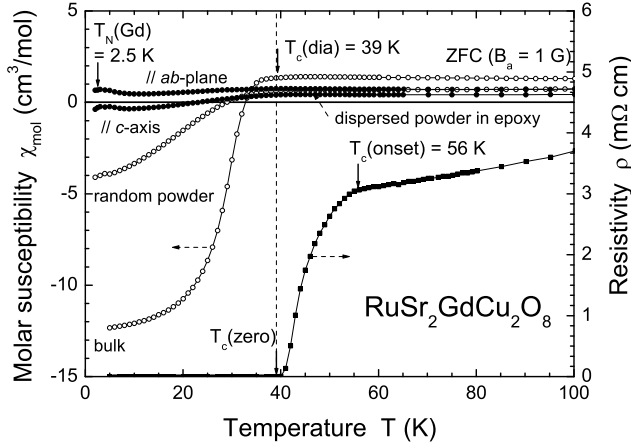


FIG. 11: Low temperature superconducting properties of aligned powder (dispersed microcrystallines in epoxy), random powder and bulk $\text{RuSr}_2\text{GdCu}_2\text{O}_8$ sample.

$T_c(\text{dia})$ of 39 K, same as the $T_c(\text{dia})$ in the bulk sample, can be clearly seen in the ZFC measurements but with a weaker diamagnetic signal. In the FC measurements, the onset of diamagnetic signal can be recognized as a kink at $T_c(\text{dia})$, the abrupt increase of magnetic signal at 30 K was attributed to the magnetic field profile inside the SQUID magnetometer⁸ and corresponds to the spontaneous vortex state temperature T_{SVS} , the same as the one observed in bulk samples.⁶ The antiferromagnetic Gd^{3+} order is observed at $T_N(\text{Gd}) = 2.5$ K.

The electrical resistivity data of bulk sample in figure 11 indicates a high superconducting onset temperature of 56 K, with a much lower $T_c(\text{zero}) = T_c(\text{dia})$ at the vortex melting temperature of 39 K. Slightly larger diamagnetic signal for random powder is probably due to partially intergrain supercurrent shielding through partial grain contact. The weak diamagnetic signal observed in aligned powder-in-epoxy samples below $T_c(\text{dia})$ is due to pure intragrain shielding with, in addition, long penetration depth λ ($\lambda_{ab} \sim 0.55 \mu\text{m}$, $\lambda_c \sim 0.66 \mu\text{m}$) in comparison with powder grain size ($\sim 1\text{-}10 \mu\text{m}$) and the two-dimensional (2D) character of CuO_2 layers.

The anisotropic high-field (± 7 T) isothermal superconducting hysteresis loops M - B_a at 100 K (Fig. 12) indicate the initial $M_{ab} > M_c$ as expected from the susceptibility. Since the magnetization curves for both field orientations showed weak-ferromagnetic behavior, the weak-ferromagnetic ordered $m(\text{Ru})$ dominates over the paramagnetic $m(\text{Gd})$ in the magnetic response and should be responsible for the complex metamagnetic-like behavior around 1 T for field applied along the ab -plane.

The magnetization curves with applied field B_a along c -axis, $M_c(B_a, T)$, and ab -plane, $M_{ab}(B_a, T)$, for aligned $\text{RuSr}_2\text{GdCu}_2\text{O}_8$ powder at 10 K are shown in Fig. 13. A strongly anisotropic magnetization was observed for

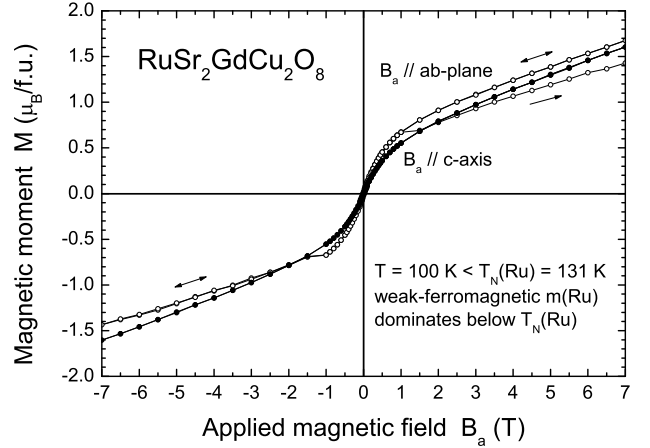


FIG. 12: Anisotropic high-field hysteresis loop $m_c(B_a)$ and $m_{ab}(B_a)$ at 100 K for aligned $\text{RuSr}_2\text{GdCu}_2\text{O}_8$ sample.

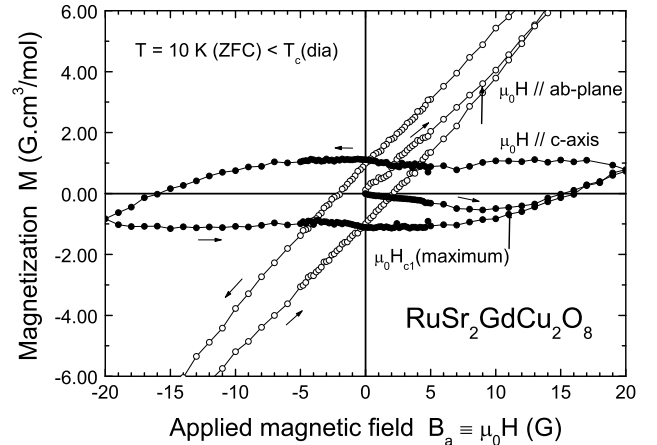


FIG. 13: Anisotropic high-field hysteresis loop $M_c(B_a)$ and $M_{ab}(B_a)$ at 10 K for aligned $\text{RuSr}_2\text{GdCu}_2\text{O}_8$ sample.

different field orientations. A superconducting hysteresis loop with a weak paramagnetic background was observed in $B_a \parallel c$ -axis with a maximum diamagnetic signal at magnetization peak field $\mu_0 H^c(\text{peak})$ of 11 G. However, no superconducting diamagnetic signal was directly observed for the initial magnetization curve for field applied along ab -plane due to the much stronger paramagnetic-like background. After subtracting the paramagnetic-like background, the maximum diamagnetic signal for M_{ab} can be obtained as $\mu_0 H^{ab}(\text{peak}) = 9$ G. The great difference of magnetization anisotropy between 100 K and 10 K observed cannot be explained by simple superposition of magnetic and superconducting components that suggests complicated interplay between the doped electrons in weak-ferromagnetically ordered RuO_6 layers and

superconducting holes in CuO_2 -layers.

IV. CONCLUSION

Anisotropic powder alignment is achieved for $\text{RuSr}_2\text{RCu}_2\text{O}_8$ weak-ferromagnetic superconductors ($R = \text{Eu}, \text{Gd}, \text{and Gd}_{0.5}\text{Dy}_{0.5}$). Due to spin-orbital related short-range anisotropic exchange interaction, paramagnetic susceptibility $\chi_{ab}(\text{Ru}/\text{Cu}) > \chi_c(\text{Ru}/\text{Cu})$ at 300 K in $\text{RuSr}_2\text{GdCu}_2\text{O}_8$ and $\text{RuSr}_2\text{EuCu}_2\text{O}_8$, c -axis aligned powder can be achieved only using field-rotational method. Total $\chi_{ab} < \chi_c$ at room temperature is dominated by R^{3+} . Due to long-range Ru anisotropic exchange interaction, total $\chi_{ab} > \chi_c$ were

observed below crossover temperature ~ 185 K, with weak-ferromagnetic $T_N(\text{Ru}) = 131$ K, superconducting $T_c(\text{dia}) = 39$ K and $T_N(\text{Gd}) = 2.5$ K. Weak diamagnetic signal observed below $T_c(\text{dia})$ was due to pure intragrain shielding with long penetration depth λ ($\lambda_{ab} \sim 0.55 \mu\text{m}$, $\lambda_c \sim 0.66 \mu\text{m}$) and the two-dimensional (2D) character of CuO_2 layers.

Acknowledgments

This work was supported by the National Science Council of R.O.C. under contract Nos. NSC95-2112-M-007-056-MY3, NSC95-2112-M-032-002, and NSC97-2112-M-003-001-MY3.

* Electronic address: hcku@phys.nthu.edu.tw

¹ L. Bauernfeind, W. Widder, and H. F. Braun, *Physica C* **254**, 151 (1995).

² C. Bernhard, J. L. Tallon, Ch. Niedermayer, Th. Blasius, A. Golnik, E. Brücher, R. K. Kremer, D. R. Noakes, C. E. Stronach, and E. J. Ansaldo, *Phys. Rev. B* **59**, 14099 (1999).

³ C. W. Chu, Y. Y. Xue, S. Tsui, J. Cmaidalka, A. K. Heilman, B. Lorenz, and R. L. Meng, *Physica C* **335**, 231 (2000).

⁴ Y. Tokunaga and H. Kotegawa and K. Ishida and Y. Kitaka and H. Takagiwa and J. Akimitsu, *Phys. Rev. Lett.* **86**, 5767

(2001).

⁵ C. Y. Yang, B. C. Chang, H. C. Ku, and Y. Y. Hsu, *Phys. Rev. B* **72**, 174508 (2005), and references cited therein.

⁶ B. C. Chang, C. Y. Yang, Y. Y. Hsu, B. N. Lin, and H. C. Ku AIP conference proceeding **850**, 677 (2006).

⁷ J. D. Jorgensen, O. Chmaissem, H. Shaked, S. Short, P. W. Klamut, B. Dabrowski, and J. L. Tallon, *Phys. Rev. B* **63**, 054440 (2001).

⁸ T. P. Papageorgiou, E. Casini, H. F. Braun, T. Herrmannsdorfer, A. D. Bianchi, and J. Wosnitza, *Euro. Phys. J. B* **52**, 383 (2006).